Title: Decreased K_{ATP} channel activity contributes to the low glucose threshold for insulin secretion in the early postnatal period

Authors: Juxiang Yang[1], Batoul Hammoud[1], Changhong Li[1], Abigail Ridler[1], Daphne Yau[1], Junil Kim[2], Kyoung-Jae Won[2], Charles A. Stanley[1,3], Toshinori Hoshi[4*], and Diana E. Stanescu[1,3*]

Affiliations:

[1] Division of Endocrinology and Diabetes, The Children's Hospital of Philadelphia, Philadelphia, PA

[2] Biotech Research & Innovation Centre, University of Copenhagen, Denmark

[3] Department of Pediatrics, Perelman School of Medicine, University of Pennsylvania, Philadelphia, PA

[4] Department of Physiology, Perelman School of Medicine, University of Pennsylvania, Philadelphia, PA

*co-corresponding authors

Corresponding authors contact information:

Toshinori Hoshi, PhD

Postal address: 415 Curie Blvd, 605 Clinical Research Building, Philadelphia, PA, 19104

Email: hoshi@pennmedicine.upenn.edu; Telephone: +1 (215) 573 7305

Diana E. Stanescu, MD

Postal address: 3615 Civic Center Blvd, 802G Abramson Research Center, Philadelphia, PA, 19104

Email: stanescud@chop.edu; Telephone: +1 (267) 425 1982

Declaration of interest: none

Abstract:

Objective: Transitional hypoglycemia in normal newborns occurs in the first 3 days of life and has clinical features consistent with hyperinsulinism. We hypothesized that this transitional hyperinsulinism is due to the persistence of a fetal lower glucose threshold for insulin release from β-cells into the first postnatal days.

Methods: We tested dynamic insulin secretion from freshly isolated rat islets between late gestation and adult age and from rat islets kept in culture for 1 or 2 days. We used single-cell transcriptomic and electrophysiology approaches to investigate the mechanism for insulin secretion at low glucose concentrations.

Results: We found that a lower threshold for glucose-stimulated insulin secretion (GSIS) is present in embryonic day (E)22 islets and persists into the first postnatal days. The glucose threshold increases in the postnatal period and reaches the adult level by postnatal day (P)14. We also demonstrated that culturing P14 islets for 24-48 hrs can also decrease the glucose threshold. Insulin release in response to BCH, a non-metabolizable leucine analog activating glutamate dehydrogenase, had a similar lower threshold in P1 compared to P14 islets. This showed that the low threshold for GSIS is determined at a step downstream of the glycolytic pathway. P1 islets had lower insulin release in response to tolbutamide, an inhibitor of β-cell K_{ATP} channels, compared to P14 islets, suggesting that decreased K_{ATP} channel expression and/or function could be responsible for the lower glucose threshold for insulin secretion. Single-cell transcriptomic analysis did not reveal differences in transcripts between E22 and P14 β-cells supporting the lower glucose threshold. The investigation of electrophysiological characteristics of dispersed β-cells showed that early neonatal cells and cultured islet cells had fewer functional K_{ATP} channels per unit membrane area.

Conclusion: These findings suggest that decreased surface density of K_{ATP} channels may contribute to the observed differences in glucose threshold for insulin release.

Key words: hypoglycemia, β-cells, neonatal, glucose threshold

1. Introduction

Transitional neonatal hypoglycemia occurs in healthy newborns in the first days of life. Plasma glucose concentrations reach a nadir by 2 hrs after birth, to a mean of 55-65 mg/dl (3-3.6 mmol/L), and increase to above 70 mg/dl (3.8 mmol/L) after the first 2-3 days, regardless of delayed or early feeding of neonates[1-4]. Clinical features suggesting hyperinsulinemic hypoglycemia during the first postnatal day include hypoketonemia, non-suppressed plasma insulin concentrations, and inappropriately large glycemic response to glucagon or epinephrine (as reviewed in [5]). A similar timing of hypoglycemia occurs in rodent models, where insulin also appears to be secreted at low glucose concentrations postnatally [6, 7]. While transitional neonatal hypoglycemia is most often mild, its underlying mechanism is unknown. Furthermore, there are few clinical criteria to differentiate it from severe or persistent forms of hypoglycemia, which can cause irreversible brain injury and long-term neurologic defects.

Fetal plasma glucose concentrations closely follow maternal plasma concentrations[8]. However, since maternal insulin does not cross the placenta, fetal β-cells are solely responsible for the fetal serum insulin level, a major growth factor during the intrauterine period. If insulin secretion or signaling is impaired, fetal growth is restricted[9, 10]. If fetal β-cells have the same glucose threshold for GSIS as adult β-cells, fetal insulin secretion would be easily suppressed and fetal growth would be impaired. Hence, a β-cell adaptation that lowers the threshold for responding to glucose may be required to allow the fetus to secrete sufficient insulin to maintain growth. The clinical features of hyperinsulinemic transitional neonatal hypoglycemia are consistent with the concept that the low fetal glucose threshold for insulin secretion persists into the early neonatal period.

We aimed to characterize the glucose threshold for insulin secretion during the fetal and early neonatal period and to uncover the mechanism underlying the hyperinsulinism causing transitional neonatal hypoglycemia. We describe here the change in glucose threshold from late embryonic period to adulthood in rats and show that decreased K_{ATP} channel function,

potentially through changes in K_{ATP} channel trafficking to the plasma membrane, is a major factor that contributes to the lower glucose threshold of embryonic and neonatal β-cells.

2. Methods

2.1. Animals: All animal experiments were performed in rats at the Children's Hospital of Philadelphia with IACUC approval. Pregnant Sprague Dawley rats at embryonic day (E)15 or E17 were purchased from Charles River Laboratories (Wilmington, MA). Dams and pups were housed together in AAALC approved rodent colony. Male and female pups were batched together for measurements. Plasma glucose concentrations were determined using a Contour Next glucose meter (Ascensia Diabetes Care, NJ).

2.2. Islet isolation and islet perifusions: Islet isolation was performed as previously described [11]. In brief, pancreases were collected at E22 (last day of gestation in rats), postnatal day (P)1, P3, P7, P14, and P28 rats of both sexes. Pancreases were digested with collagenase (Millipore Sigma, Burlington, MA) in Hank's buffer. Islets were handpicked twice and then incubated in regular islet media (RPMI 1640, supplemented with 5 mM glucose, 10% fetal bovine serum, 2 mM glutamine, 1% antibiotics (Gibco, Gaithersburg, MD)) at 37°C for 3 hrs or, in some experiments, for 1 or 2 days, as specified. Islets, 200-250, isolated from 1-5 rat pups, depending on postnatal age, were perifused at a flow rate of 1 ml/min. Perifusion media was a Krebs-Ringer bicarbonate buffer supplemented with 0.25% bovine serum albumin and 2 mM glutamine. Because of the low rates of insulin secretion in fetal islets, perifusion media was also supplemented with 0.1 mM 3-isobutyl-1-methylxanthine (IBMX), a phosphodiesterase inhibitor to augment Ca^{2+}-stimulated insulin secretion and bring insulin measurements in the range of the insulin assay. After 30 min of perifusion with glucose-free buffer, step-wise increasing concentrations of glucose, BCH (2-aminobicyclo-(2,2,1)-heptane-2-carboxylic acid) or tolbutamide were added, every 20 min, as described in the figures. After return to basal conditions for another 20 min, islets were exposed to 30 mM KCl to determine maximal insulin release at the end of the perifusion. Samples were collected every min for insulin assay using Insulin High Range Kits (Cisbio Assays, Bedford, MA) following the manufacturer's instructions.

For representation in Figures 1-3, % insulin release per min in response to glucose, BCH or tolbutamide is calculated as percentage of maximal KCl-stimulated insulin release for each replicate in each condition. Data points are connected with straight lines for presentation clarity only.

2.3. Single-cell sequencing and analysis: Islets were isolated as described above from E22 embryos and P14 pups of both sexes. Islets were washed once with PBS without Mg^{2+} and Ca^{2+}, followed by dissociation with TripLe (Gibco, Gaithersburg, MD) for 7-9 min with gentle pipetting every 1 min. Dissociation was stopped by adding fetal bovine serum. The cell mixture was immediately filtered through 40 µm cell strainer, washed three times with cold PBS, and resuspended in regular islet media (as above). Single-cell suspensions were visualized under a microscope to assess cell viability and to ensure an adequate concentration for single-cell preparation. Cells were loaded on the 10X Genomics Chromium Controller (Pleasanton, CA) in the Center for Applied Genomics at CHOP, as per manufacturer's instructions. Single-cell transcriptome libraries were sequenced on the HiSeq platform (Illumina, San Diego, CA). The CellRanger (v.2.1,10x genomics) pipeline was used for barcode filtering, alignment to *Rattus norvegicus* genome and Unique Molecular Identifiers (UMI) counting. Sequenced 10x libraries were individually evaluated using multiple criteria to determine cells of interest, including gene number (200 – 3000), number of UMI(0 – 20000), and percent mitochondrial gene expression (<0.10). The top 10 principal components were used to perform clustering and visualization using a t-distributed stochastic neighbor embedding (tSNE) plot. Gene marker expression was used to identify specific populations. We sequenced a total of 3556 cells, of which we identified 1072 cells (237 from E22 embryos and 835 from P14 pups) with transcriptomic signatures expected of β-cells (Suppl Fig. 2). List of differentially expressed genes between E22 and P14 β-cells is provided in Supplemental Table.

2.4. Whole-cell patch-clamp measurements: Electrophysiological measurements were performed using the apparatus previously described [12]. Membrane potentials (V_m) were monitored using the perforated whole-cell patch-clamp method with β-escin (MP Biomedicals, Santa Ana, CA) as the perforating agent (6 to 8 μM). The extracellular solution contained (in mM): 135 NaCl, 4 KCl, 2 $CaCl_2$, 2 $MgCl_2$, 10 mannitol, 5 glucose, 10 HEPES, pH 7.2 with *N*-methyl-*D*-glucamine (NMG). The intracellular solution contained (in mM): 76 K_2SO4, 10 KCl, 10 NaCl, 6 $MgCl_2$, 30 mannitol, 30 HEPES, pH 7.2 with NMG. Accounting for the divalent cation-chelating action of SO_4^{2-}, the free Mg^{2+} concentration is estimated to be ~2 mM. The tip of the wax-coated electrode was filled with the intracellular solution and back-filled with the β-escin-containing intracellular solution. The current-clamp measurements were performed under a continuous perfusion condition (0.3 to 0.4 mL/min) at 35 °C (Warner TC-124A and TC-344B, Holliston, MA).

Voltage-clamp measurements were performed in the whole-cell configuration patch-clamp method at room temperature. Wax-coated patch electrodes (Warner G85150T) had a typical initial input resistance of 2 to 4 Mohms using the solutions described below. The external bath solution contained (in mM): 140 KCl, 2 MgCl2, 10 HEPES, pH 7.2 with *N*-methyl-*D*-glucamine (NMG). The internal pipette solution contained (in mM): 140 KCl, 11 EGTA, 10 HEPES, pH 7.2 with NMG. Once a gigaohm seal was obtained, the cell was transferred to a small perfusion chamber, ~150 μl n size, and then the membrane within the patch electrode was ruptured by negative pressure to obtain the whole-cell configuration. The cell was held at 0 mV and short 10 mV-square pulses were first applied to estimate total membrane capacitance and input resistance. Following electronic compensation for the capacitance and series resistance (~60%), voltage ramps from –80 mV to 80 mV in 400 ms were applied every 12 s. After establishing the whole-configuration, currents often increased in size, presumably because of loss intracellular components such as ATP, and the currents stabilized within 4 to 5 min, after which glyburide (400 nM; Sigma), a K_{ATP} channel inhibitor, was applied. Once the currents were

stable in size in the presence of glyburide, the broad-spectrum K^+ channel inhibitor quinidine (200 μM) was added to assess the gigaohm seal integrity. In some experiments, currents were recorded for up to 12 min before glyburide was applied to ensure that there was no slow change in current size, which was not observed.

The dissociated cells were amenable to electrophysiological measurements for up to 2 hrs following the cell isolation procedure. All salts were from Sigma (MilliporeSigma, Burlington, MA). The V_m values shown have been corrected for the junction potential.

3. Results

3.1. Glucose threshold for insulin secretion is lower in fetal and early postnatal islets.

Figure 1A compares the insulin response of islets from E22 embryos, P1, P3, P7 and P14 pups, and adult rats to stepwise glucose-stimulated insulin secretion (GSIS) from 3 to 25 mM. Glucose threshold was defined as the lowest glucose concentration examined at which insulin release exceeded 10% of the maximal release by 30 mM KCl above basal. The E22 islets showed a glucose threshold at 3 mM glucose. P1-P7 islets exhibited a progressive rightward shift in the glucose threshold with diminishing responses to 3 mM and then to 5 mM glucose until reaching a threshold of 10 mM in P14 and adult islets; P14 and adult rat islets released insulin only at the 10 mM glucose step or above. In E22 islets and at all other ages, the maximum insulin response to glucose in the presence of IBMX was similar to the response to membrane depolarization with KCl. The increase in threshold for GSIS closely paralleled the increase in plasma glucose concentrations between P1 to P14 (Fig. 1B). These observations are consistent with the hypothesis that transitional neonatal hypoglycemia in human newborns is due to a lower fetal glucose threshold for GSIS, which is maintained in the immediate postnatal period. [5]

3.2. The low glucose threshold in neonatal islets reflects differences in the insulin secretory pathway distal to glycolysis.

To assess whether the low glucose threshold for insulin release in fetal and newborn islets was determined within the glycolytic pathway, we examined the responses of P1 and P14 islets to increasing concentrations of BCH, a non-metabolizable leucine analog. BCH promotes insulin release by activating β-cell mitochondrial glutamate dehydrogenase to stimulate oxidation of glutamate via α-ketoglutarate, leading to a rise in β-cell ATP/ADP ratio and triggering insulin secretion[13]. As shown in Fig. 2A, the BCH threshold for insulin secretion was lower in P1 islets (1 mM) compared to P14 islets (3 mM), suggesting that the low glucose

threshold for insulin release in fetal and neonatal islets is determined at a step downstream of the glycolytic pathway.

To examine steps distal to mitochondrial ATP production, we assessed insulin responses to tolbutamide, an inhibitor of β-cell K_{ATP} channels that causes plasma membrane depolarization to trigger influx of Ca^{2+} and subsequent insulin release. The insulin response was markedly lower at all concentrations of tolbutamide in P1 islets compared to P14 islets, despite similar maximal insulin responses to KCl depolarization (Fig 2B). This observation suggested that K_{ATP} channel activity and/or channel surface expression is lower in P1 than in P14 islets because a similar pattern of insulin secretion is seen in SUR1 knock-out islets, which have reduced insulin response to K_{ATP} channel inhibitors, but normal response to KCl [14-16].

3.3. Culturing islets lowers the glucose threshold for insulin secretion.

Davis and Matschinsky have previously shown that culturing human islets for 48 hrs decreased the glucose threshold for insulin secretion from 4-5 mM down to 2-3 mM [17]. We confirmed this observation in rat P14 islets: culturing for 1 or 2 days decreased the glucose threshold from 10 mM to 3 mM (Fig. 3A , Suppl. Fig. 1A). In contrast, for P1 islets, which already had a lower glucose threshold, 2 days of culture did not change the glucose threshold for insulin release (Suppl. Fig. 1B). The insulin response to the K_{ATP} channel inhibitor tolbutamide was similarly diminished in P14 islets cultured for 2 days (Fig. 3B, C) and also in freshly isolated P1 islets (Fig. 2B). These findings show that P14 cultured islets have diminished responses to tolbutamide and implicate changes in the insulin secretory pathway β-cells at the closure of K_{ATP} channels.

3.4 Single-cell transcriptomic analysis of E22 and P14 cells.

We performed differential expression analysis of single E22/P14 β-cells to identify gene transcript changes that could influence the glucose threshold for GSIS. We identified 237 β-cells

from E22 embryos and 835 β-cells from P14 pups (Suppl. Fig. 2A-B); 135 transcripts were upregulated in E22 β-cells but only 17 transcripts were upregulated in P14 β-cells (false discovery rate <0.0001, logRatio>0.3) (Suppl. Fig. 2D; Suppl. Table). β-cell maturational markers, such as *MafB, Npy* and *Nnat*, were upregulated in E22 β-cells compared to P14 β-cells, consistent with previous reports [6, 18, 19](Suppl. Fig. 2E). Among top upregulated genes in the P14 β-cells were *Sfrp5, Syt4, Ppy, Dbp* and *Pcsk1n* (Suppl. Fig. 2E, Suppl Table).

Several factors upstream of mitochondrial oxidation, including lactate dehydrogenase *(Ldh),* monocarboxylic transporter 1 *(Slc16a1),* and hexokinase isoforms 1-3 *(Hk1-3),* have been suggested to be responsible for the low glucose threshold for GSIS of early postnatal β-cells [20-22]. These transcripts were not differentially expressed between the rat E22 and P14 β-cells. The lack of transcriptional changes, in the context of the perifusion data presented above, shows that these factors may not be responsible for the low glucose threshold in fetal and neonatal islets.

The above studies of BCH-stimulated and tolbutamide-stimulated insulin secretion suggested that decreased activity or expression of K_{ATP} channels, comprised of $K_{ir}6.2$ channels complexed with sulfonylurea receptors (SUR1), could be responsible for the lower glucose threshold of fetal and neonatal β-cells (see Fig. 2B). However, the mRNA level of *Abcc8* (SUR1) was higher in E22 β-cells and no difference in *Kcnj11* transcript ($K_{ir}6.2$) was detected (Suppl. Fig. 2E). This suggested that decreased transcription of K_{ATP} channel subunit genes is not the cause of the lower glucose threshold in neonatal islets.

3.5. Neonatal islet cells have fewer functional K_{ATP} channels.

The β-cell membrane potential (V_m), in part controlled by K_{ATP} channels, is a critical regulator of insulin release [23]. The lower glucose threshold in the fetal and early neonatal islets suggested the possibility that these β-cells have a V_m closer to the level at which voltage-dependent Ca^{2+} channels open to allow Ca^{2+} influx and subsequent insulin release. To test this

prediction, we measured V_m values in individual cells from P3 and P14 islets incubated with 5 mM glucose. These two age groups were selected because the P3 islets were readily identified and amenable to enzymatic dissociation, whereas islets from younger animals were difficult to dissociate while maintaining their functionality. In addition, as shown in Fig 1A, at 5 mM glucose, P3 islets exhibited ~40% of maximal insulin release while P14 islets essentially showed no insulin release, rendering comparison easy. V_m sweeps recorded from 29 cells isolated from 6 P3 pups and 33 cells from 9 P14 pups are illustrated in Fig. 4A. The V_m values show a high degree of variability in each group, ranging from near –90 mV to –30 mV (Fig. 4A; Suppl. Fig. 3). Many of the cells exhibited non-over-shooting action potentials (APs) typical of β-cells (Suppl. Fig. 3). We observed that 18% of P3 cells had V_m values ≥ –60 mV cells compared with 41% in P14 cells (Fig. 4A). This greater fraction of depolarized cells in the P3 group could contribute to the lower glucose threshold for GSIS found in the younger islets. While we do not have clear information regarding the cell-type identity of each cell in our electrophysiological measurements, in those experiments in which the glucose concentration was increased from 5 to 25 mM, the cells responded by firing non-overshooting APs, as expected from functionally viable β-cells (Suppl. Fig. 3).

Plasma membrane depolarization in β-cells may be facilitated by closure/inhibition of K_{ATP} channels and/or a reduced number of channels trafficked to the cell surface [23, 24]. Our perifusion results suggested that reduced K_{ATP} channel number or activity could contribute to the observed differences in the glucose threshold, both between E22-P14 islets and with culturing islets for 1 or 2 days. Total membrane currents under a symmetrical 140 mM KCl condition were recorded from 20 P3 uncultured neonatal islet cells, 13 P14 uncultured islet cells, and 20 P14 islet cells cultured for 2 days. Input capacitance, reflecting the membrane area, was similar for uncultured P3 and P14 cells, and slightly greater the P14 cultured group (Suppl. Fig. 4A). After establishing the whole-cell configuration, currents in response to repeated voltage ramps were recorded and illustrative results from a P14 cell are depicted in Suppl. Fig. 4B. The whole-cell

configuration, establishing a small conduit through the membrane, disrupts the cellular enzymatic machinery. Therefore, the ramp currents immediately following establishing the whole-cell configuration reflect the near physiological ion channel status and those recorded later in time represent very compromised biochemical conditions when the ATP content is low (Suppl. Fig. 4B; Suppl. Fig. 5A-B). Glyburide (400 nM) was next applied to inhibit K_{ATP} channels (Suppl. Fig. 4B; Suppl. Fig. 5C) and then quinidine, a broad-spectrum K^+ channel inhibitor, was applied to assess the gigaohm seal integrity (Suppl. Fig. 4B; Suppl. Fig. 5D). The currents immediately after achieving the whole-cell configuration (~30 s) were noticeably greater in the uncultured P14 cells than in uncultured P3 or cultured P14 cells (Suppl. Fig 5A). In most of the cells, the currents increased in size with time after achieving the whole-cell configuration, especially in P14 cells, probably due to disruption of ATP supply which activated K_{ATP} channels (Suppl. Fig. 5B). The currents were subsequently nearly entirely blocked by the K_{ATP} channel inhibitor glyburide (Suppl. Fig. 5C), suggesting that K_{ATP} channels dominate the whole-cell currents.

Cultured P14 cells appeared to be comprised of two subpopulations based on the glyburide-sensitivity, with 60% (14 out of 20) of cultured P14 cells having no appreciable glyburide-sensitive currents (Fig. 4C – *green* circles). Uncultured P3 cells presented a similar two subpopulation distribution, with some of the cells exhibiting decreased glyburide-sensitive K^+ currents compared to the uncultured P14 cells (Fig. 4C – *red* circles vs. *blue* circles). Thus, both P3 and cultured P14 islet cells had decreased glyburide-sensitive K^+ currents, very likely K_{ATP} currents. These findings collectively suggest that decreased K_{ATP} channel activity, potentially due to decreased trafficking of channels to the plasma membrane, is the main contributor to the lower glucose threshold for GSIS in neonatal and cultured β-cells.

4. Discussion

The results of these studies demonstrate that fetal and early neonatal pancreatic β-cells respond to glucose stimulation with a lower glucose threshold than mature β-cells. This low threshold for GSIS correlates closely with the period of transitional hypoglycemia in normal newborns during the first day after birth. Our results further show that the differences in glucose threshold for GSIS during this period reflect changes distal to glycolysis and appear to involve the triggering pathway for insulin secretion at the site of the plasma membrane K_{ATP} channel. Electrophysiological measurements reveal reduced K_{ATP} channel activity, reflecting decreased density on the plasma membrane of neonatal β-cell. Culturing of isolated islets for 1-2 days produced a similar effect of reduced glucose threshold and reduced K_{ATP} activity, suggesting the possibility that extrinsic rather than developmental factors may be responsible for transitional neonatal hypoglycemia.

The glucose threshold for GSIS, which determines the basal concentration of plasma glucose, is controlled by numerous components of the insulin secretory pathway, from the initial step of glucose phosphorylation to distal steps of insulin vesicle exocytosis. While glucokinase functions as the β-cell glucose sensor, mutations in many of the subsequent steps in the pathway of insulin secretion have been found to lead to either diabetes or hyperinsulinism[25]. Several of these involve K_{ATP} channel gene expression or activity, reflecting the key role of this channel in insulin regulation. Loss of function mutations in K_{ATP} channel subunits, *KCNJ11* and *ABCC8*, lead to congenital hyperinsulinemic hypoglycemia due to a failure to appropriately suppress insulin release, while gain-of-function K_{ATP} mutations cause monogenic diabetes [26-28]. Decreased gene expression of K_{ATP} channel subunits has also been proposed to be responsible for the infantile hyperinsulinemic hypoglycemia and subsequent maturity onset diabetes associated with inactivating mutations of HNF1A and HNF4A transcription factors [29-32]. Recently, the mechanism of decreased insulin secretion induced by leptin has been shown to involve increased density of K_{ATP} channels on the plasma membrane surface due to

increased trafficking of channels[33]. Conversely, a defect in this leptin response pathway in PHPT1$^{-/-}$ mice causes lethal neonatal hypoglycemia due to impaired trafficking and decreased surface density of K_{ATP} channels.[24]

Several mechanisms have been suggested to explain the lower glucose threshold of neonatal islets: increased expression of genes disallowed in mature β-cells (*Slc16a1*, *LDH* genes and hexokinase isoforms with low affinity for glucose) or decreased expression of *Syt4* leading to increased sensitivity of insulin vesicles to Ca^{2+}[7, 20-22]. We conclude here that the aforementioned mechanisms are unlikely to play a major role in determining the lower glucose threshold for GSIS in rat neonatal islets for two reasons. Firstly, the low threshold for BCH-stimulated insulin secretion suggests that the low glucose threshold is determined at a step downstream of mitochondrial oxidation. This finding is in accord with the observed lack of transcript level changes in *Hk1-3, Slc16a1* or *LDH* between E22 and P14 β-cells. Secondly, we have shown that *Syt4* expression is lower in E22 compared to P14 β-cells, supporting the role of this factor in the postnatal β-cell functional changes[7]. However, the resulting increase sensitivity of insulin granules to Ca^{2+} due to lower Syt4 expression in fetal and early neonatal β-cells would predict an increased, not a decreased, tolbutamide-stimulated insulin secretion from early neonatal islets.

Our single-cell transcriptomic analysis failed to detect transcriptomic-level regulation of *Kcnj11* or *Abcc8* genes between E22 and P14, consistent with other similar single-cell or bulk transcriptomic data sets in mice [18, 34]. This suggested that decreased K_{ATP} channel surface density in fetal and neonatal β-cells contributes to the low glucose threshold for GSIS, leading to transitional hypoglycemia in the early neonatal period. We thus postulate that the change in K_{ATP} current size is due to decreased channel trafficking to plasma membrane.

Fetal islets have poor maximal insulin responses to glucose stimulation and a higher maximal response to amino acids [6, 35-37]. The poor responsiveness to glucose has been attributed to limitations in the glycolytic pathway or to impairments in mitochondrial oxidation of

glucose [34, 38]. It has also been suggested that limitations in glucose response are correlated with β-cell differentiation and/or proliferation[39]. Although the experiments here did not attempt to address these concepts, our observation of reduced K_{ATP} channel activity may not only explain the low glucose threshold for GSIS of fetal islets but also their limited maximal GSIS and increased responsiveness to amino acids. Similar limitation of maximal GSIS and increased responsiveness to amino acids are seen in genetic deficiency of K_{ATP} channels in infants and in rodents [11, 16, 40, 41]. In islets with impaired K_{ATP} channels, the insulin-glucose response curve is flattened with incomplete suppression of insulin release at low glucose concentrations and diminished rise in insulin at high glucose concentrations.[16] Human and mouse islets with K_{ATP} mutations also show an exaggerated response to a mixture of amino acids via the amplification pathway in the presence of elevated concentrations of cytosolic Ca^{2+}.[16, 41]

The lower glucose threshold for GSIS of cultured islets, previously observed in isolated islets that had been cultured for 48 hrs[17], can be explained by our finding here that 60% of cultured β-cells have markedly reduced glyburide-sensitive K^+ currents. The fact that fetal/neonatal islets and islets exposed to culture conditions share a similar low glucose threshold for GSIS suggests the possibility of similar underlying mechanisms driven by extrinsic factors, such as exposure to hypoxia or constant nutrient supply, rather than a programmed maturational process. The interior of cultured islets has reduced oxygen and a continuous nutrient supply[42]. The fetal environment is also characterized by low oxygen concentrations and more severe restriction of fetal oxygen or nutrient supply, as in birth asphyxia or late intrauterine growth retardation, is known to cause perinatal stress-induced hyperinsulinism that may persist for several weeks after delivery [43, 44]. It is thus possible that changes in the mTOR/AMP-kinase [35] and/or the hypoxia-inducible factor pathways could signal the postnatal increase in K_{ATP} channel trafficking to the β-cell plasma membrane and the increase threshold for GSIS.

In conclusion, we have established that fetal and early postnatal β-cell function are characterized by a low glucose threshold for GSIS. This low threshold correlates with decreased K_{ATP} channel surface density. These findings support the concept that transitional neonatal hypoglycemia represents an extension into the early postnatal period of the fetal pattern of insulin release from β-cells.

Acknowledgements and funding: We thank Dr. Franz Matschinsky for critical review of the manuscript. We also thank the Center for Applied Genomics at The Children's Hospital of Philadelphia. DES was supported by American Diabetes Association Junior Faculty Development Award (1-16-JDF086). CAS was supported by NIH grant R37-DK056268. TH was supported in part by NIH GM121375 and DK098517.

Data availability statement: raw single cell transcriptomic data will be available upon request from DES.

Author contributions: JY, BH designed and performed experiments, interpreted the results with input from DES and wrote parts of the manuscript. CL designed and performed experiments, interpreted the results, contributed to the conceptual frame work. AR performed experiments and revised the manuscript. DY designed and performed experiments. JK performed the bioinformatic analysis, interpreted the data. KJW conceptualized the bioinformatic analysis and revised the manuscript. CAH conceptualized and supervised the project, wrote and edited the manuscript. TH conceptualized the electrophysiological approach, performed experiments, interpreted the data and wrote/edited the manuscript. DES conceptualized and supervised the project overall, analyzed the data, wrote/edited the manuscript.

Figure Legends:

Figure 1: The glucose threshold for GSIS increases in early postnatal rat islets. A. Islet perifusions with stepwise increases in glucose concentrations from 3 to 25 mM followed by 30 mM KCl for each age as depicted. Insulin release per min is calculated as percentage of maximal KCl-stimulated insulin release for each replicate. A total of 3-5 independent pools of islets (200-250 islets each) were obtained from 1-5 animals for each age. **B.** Plasma glucose concentrations of rat pups between 1-28 days of age. Each point represents measurements of one pup. Error bars in **A** and **B** represent SEM.

Figure 2: The lower threshold for insulin secretion is determined by changes in the distal steps of insulin secretion pathway. A: Perifusions with stepwise increases in BCH concentration from 1 to 10 mM followed by 30 mM KCl in P1 and P14 freshly isolated rat islets. **B:** Perifusions with stepwise increases in tolbutamide concentration from 25 to 150 μM in freshly isolated P1 and P14 rat islets. Insulin release per min is calculated as percentages of maximal KCl-stimulated insulin secretion for each replicate and age. Three independent pools of islets (200-250 islets each) were obtained from 1-5 animals for each age. Error bars represent SEM.

Figure 3: Glucose threshold for insulin release decreases after 2 days of islet culture. A: Perifusions with stepwise increases in glucose concentration from 3 to 25 mM followed by 30 mM KCl in freshly isolated P14 islets or P14 islets that had been cultured for 2 days. **B:** Perifusions with stepwise increases in tolbutamide concentration from 25 to 150 μM in freshly isolated islets and P14 islets that had been cultured for 2 days. **C:** Tolbutamide response curve in freshly isolated P1 or P14 islets and cultured P14 islets. For **A-B**, 3-4 independent pools of islets (200-250 islets each) were obtained from 1-5 animals for each age. Insulin release per min is calculated as percentages of maximal KCl-stimulated insulin secretion for each replicate and age. Error bars represent SEM.

Figure 4: Electrophysiological differences between P3 and P14 rat islet cells. A-B P3 rat cells have a more depolarized membrane potential (V_m) at 5 mM glucose compared with P14 cells**. A**. Compressed 60-sec recordings of V_m values for each cell represented on the *x* axis: 29 P3 islet cells (*left*, red) and 33 P14 islet cells(*right*, blue). **B**. Probability density functions of median V_m values from the cells in P3 cells (*left*, red) and P14 cells (*right*, blue). **C**. Uncultured P3 cells and cultured P14 cells have smaller glyburide-sensitive currents than uncultured P14 cells. Glyburide-sensitive currents normalized by cell capacitance at –80 mV for each cell measured. Each cell is represented by a circle. Statistical analysis: One Way ANOVA (Kruskal Wallis) p-value is 0.002; Mann-Whitney test for comparing two groups: (*) P3 no culture vs P14 no culture: p = 0.032, (**) P3 no culture vs P14 culture: p = 0.01, (***) P14 culture vs P14 no culture: p= 0.003.

Supplemental Fig 1: Islet perifusions with stepwise increases in concentrations of glucose for P14 islets that had been cultured for 1 day(**A**) and for P1 islets that had been cultured for 2 days (**B**). Insulin release per min is calculated as percentages of maximal KCl-stimulated insulin release for each replicate. Three independent pools of islets were obtained from 1-5 animals for each age, for a total of 100-200 islets/replicate. Error bars represent SEM.

Supplemental Fig 2: Single cell transcriptomic analysis: A-B. t-SNE representation of E22/P14 isolated pancreas cells. **A:** Different clusters were identified based on expression of cell-specific genes. **B:** Cells are labeled depending on the age: E22 cells are presented in dark gray and P14 cells are represented in red. **C.** Expression of specific markers in distinct clusters on the t-SNE plot, leading to the identification of cell types. **D.** Heatmap of differentially expressed genes in E22 or P14 β-cells. **E:** Violin plots of log2 normalized expression levels (FPKM) for specific transcripts in E22 or P14 β-cells.

Supplemental Fig 3: Illustration of changes in membrane potential (V_m) from two P14 islet cells in response to a step change in glucose concentration ([G]) from 5 mM to 25 mM.

Supplemental Fig 4: K^+ currents in islet cells. A. Capacitance values of individual cells for the 3 conditions. Each cell is depicted by a circle (*red* for uncultured P3 cells, *blue* for uncultured P14 cells, and *green* for cultured P14 cells). **B**. A typical experimental sequence with voltage ramp stimulations from one P14 no culture islet cell. WC = Whole-cell configuration. **C**. Current sizes at -80 mV at different times after establishing the whole-cell configuration (t = 0 s) from the experiment shown in **B**. Glyburide was applied at 400 nM and quinidine was applied at 200 μM.

Supplemental Fig 5: Currents elicited by voltage ramps normalized by cell capacitance elicited by voltage ramps in individual cells **(A)** 20 to 30 s after whole-cell configuration, (**B**) after "run-

up" of currents caused presumably by ATP loss, (**C**) after 400 nM glyburide, (**D**) after 200 μM quinidine. Results from uncultured P3 cells (*red*, *left*), uncultured P14 cells (*blue*, *center*), and cultured P14 cells (*green*, *right*). For **A**, **B**, and **C**, current sizes at –80 mV are shown (*right panels*). For **D**, the current sizes at –80 mV are not shown because the sizes are near nil in almost all cells.

Supplemental Table: List of differentially expressed genes in E22 or P14 β-cells (false discovery rate <0.0001, logRatio>0.3) Genes are listed in the order they appear in the heatmap in Supplemental Fig. 2D.

References:

1. Cornblath, M. and S.H. Reisner, *Blood glucose in the neonate and its clinical significance.* N Engl J Med, 1965. **273**(7): p. 378-81.
2. Bozzetti, P., et al., *The relationship of maternal and fetal glucose concentrations in the human from midgestation until term.* Metabolism, 1988. **37**(4): p. 358-63.
3. Hoseth, E., et al., *Blood glucose levels in a population of healthy, breast fed, term infants of appropriate size for gestational age.* Arch Dis Child Fetal Neonatal Ed, 2000. **83**(2): p. F117-9.
4. Srinivasan, G., et al., *Plasma glucose values in normal neonates: a new look.* J Pediatr, 1986. **109**(1): p. 114-7.
5. Stanley, C.A., et al., *Re-evaluating "transitional neonatal hypoglycemia": mechanism and implications for management.* J Pediatr, 2015. **166**(6): p. 1520-5 e1.
6. Blum, B., et al., *Functional β-cell maturation is marked by an increased glucose threshold and by expression of urocortin 3.* Nat Biotechnol, 2012. **30**(3): p. 261-4.
7. Huang, C., et al., *Synaptotagmin 4 Regulates Pancreatic β-cell Maturation by Modulating the Ca^{2+} Sensitivity of Insulin Secretion Vesicles.* Dev Cell, 2018. **45**(3): p. 347-361 e5.
8. Marconi, A.M., et al., *The impact of gestational age and fetal growth on the maternal-fetal glucose concentration difference.* Obstet Gynecol, 1996. **87**(6): p. 937-42.
9. Fowden, A.L., *Insulin deficiency: effects on fetal growth and development.* J Paediatr Child Health, 1993. **29**(1): p. 6-11.
10. Hill, D.J. and R.D. Milner, *Insulin as a growth factor.* Pediatr Res, 1985. **19**(9): p. 879-86.
11. Li, C., et al., *Regulation of leucine-stimulated insulin secretion and glutamine metabolism in isolated rat islets.* J Biol Chem, 2003. **278**(5): p. 2853-8.
12. Tian, Y., S.H. Heinemann, and T. Hoshi, *Large-conductance Ca^{2}+- and voltage-gated K^{+} channels form and break interactions with membrane lipids during each gating cycle.* Proc Natl Acad Sci U S A, 2019. **116**(17): p. 8591-8596.
13. Sener, A., F. Malaisse-Lagae, and W.J. Malaisse, *Stimulation of pancreatic islet metabolism and insulin release by a nonmetabolizable amino acid.* Proc Natl Acad Sci U S A, 1981. **78**(9): p. 5460-4.
14. Szollosi, A., M. Nenquin, and J.C. Henquin, *Pharmacological stimulation and inhibition of insulin secretion in mouse islets lacking ATP-sensitive K+ channels.* Br J Pharmacol, 2010. **159**(3): p. 669-77.
15. Szollosi, A., et al., *Glucose stimulates Ca2+ influx and insulin secretion in 2-week-old β-cells lacking ATP-sensitive K+ channels.* J Biol Chem, 2007. **282**(3): p. 1747-56.
16. Li, C., et al., *Functional and Metabolomic Consequences of K_{ATP} Channel Inactivation in Human Islets.* Diabetes, 2017. **66**(7): p. 1901-1913.
17. Matschinsky F.M., D.E.A., *The Distinction between 'Glucose Setpoint', 'Glucose Threshold' and 'Glucose Sensor' Is Critical for Understanding the Role of the Pancreatic B-cell in Glucose Homeostasis*. Molecular and Cell Biology of Type 2 Diabetes and Its Complications, ed. L.M. Belfiore F., Molinatti G.M., Porta M. Vol. 14. 1998, Front Diabetes. Basel: Karger. 14-29.
18. Zeng, C., et al., *Pseudotemporal Ordering of Single Cells Reveals Metabolic Control of Postnatal β-cell Proliferation.* Cell Metab, 2017. **25**(5): p. 1160-1175 e11.
19. Rodnoi, P., et al., *Neuropeptide Y expression marks partially differentiated β-cells in mice and humans.* JCI Insight, 2017. **2**(12).
20. Sekine, N., et al., *Low lactate dehydrogenase and high mitochondrial glycerol phosphate dehydrogenase in pancreatic β-cells. Potential role in nutrient sensing.* J Biol Chem, 1994. **269**(7): p. 4895-902.
21. Pullen, T.J., et al., *Identification of genes selectively disallowed in the pancreatic islet.* Islets, 2010. **2**(2): p. 89-95.

22. Thorrez, L., et al., *Tissue-specific disallowance of housekeeping genes: the other face of cell differentiation.* Genome Res, 2011. **21**(1): p. 95-105.
23. Rorsman, P. and F.M. Ashcroft, *Pancreatic β-cell Electrical Activity and Insulin Secretion: Of Mice and Men.* Physiol Rev, 2018. **98**(1): p. 117-214.
24. Srivastava, S., et al., *Regulation of K_{ATP} Channel Trafficking in Pancreatic β-cells by Protein Histidine Phosphorylation.* Diabetes, 2018. **67**(5): p. 849-860.
25. Matschinsky, F.M. and D.F. Wilson, *The Central Role of Glucokinase in Glucose Homeostasis: A Perspective 50 Years After Demonstrating the Presence of the Enzyme in Islets of Langerhans.* Front Physiol, 2019. **10**: p. 148.
26. De Leon, D.D. and C.A. Stanley, *Permanent Neonatal Diabetes Mellitus*, in *GeneReviews((R))*, M.P. Adam, et al., Editors. 1993: Seattle (WA).
27. Rosenfeld, E., A. Ganguly, and D.D. De Leon, *Congenital hyperinsulinism disorders: Genetic and clinical characteristics.* Am J Med Genet C Semin Med Genet, 2019. **181**(4): p. 682-692.
28. Hussain, K. and K.E. Cosgrove, *From congenital hyperinsulinism to diabetes mellitus: the role of pancreatic β-cell K_{ATP} channels.* Pediatr Diabetes, 2005. **6**(2): p. 103-13.
29. Flanagan, S.E., et al., *Diazoxide-responsive hyperinsulinemic hypoglycemia caused by HNF4A gene mutations.* Eur J Endocrinol, 2010. **162**(5): p. 987-92.
30. Haliyur, R., et al., *Human islets expressing HNF1A variant have defective β-cell transcriptional regulatory networks.* J Clin Invest, 2019. **129**(1): p. 246-251.
31. Stanescu, D.E., et al., *Novel presentations of congenital hyperinsulinism due to mutations in the MODY genes: HNF1A and HNF4A.* J Clin Endocrinol Metab, 2012. **97**(10): p. E2026-30.
32. Gupta, R.K., et al., *The MODY1 gene HNF-4alpha regulates selected genes involved in insulin secretion.* J Clin Invest, 2005. **115**(4): p. 1006-15.
33. Chen, P.C., Y.N. Kryukova, and S.L. Shyng, *Leptin regulates K_{ATP} channel trafficking in pancreatic β-cells by a signaling mechanism involving AMP-activated protein kinase (AMPK) and cAMP-dependent protein kinase (PKA).* J Biol Chem, 2013. **288**(47): p. 34098-109.
34. Jermendy, A., et al., *Rat neonatal β-cells lack the specialised metabolic phenotype of mature β-cells.* Diabetologia, 2011. **54**(3): p. 594-604.
35. Helman, A., et al., *A Nutrient-Sensing Transition at Birth Triggers Glucose-Responsive Insulin Secretion.* Cell Metab, 2020. **31**(5): p. 1004-1016 e5.
36. Rozzo, A., et al., *Exocytosis of insulin: in vivo maturation of mouse endocrine pancreas.* Ann N Y Acad Sci, 2009. **1152**: p. 53-62.
37. Rorsman, P., et al., *Failure of glucose to elicit a normal secretory response in fetal pancreatic β-cells results from glucose insensitivity of the ATP-regulated K+ channels.* Proc Natl Acad Sci U S A, 1989. **86**(12): p. 4505-9.
38. Taniguchi, S., K. Tanigawa, and I. Miwa, *Immaturity of glucose-induced insulin secretion in fetal rat islets is due to low glucokinase activity.* Horm Metab Res, 2000. **32**(3): p. 97-102.
39. Puri, S., et al., *Replication confers β-cell immaturity.* Nat Commun, 2018. **9**(1): p. 485.
40. Grimberg, A., et al., *Dysregulation of insulin secretion in children with congenital hyperinsulinism due to sulfonylurea receptor mutations.* Diabetes, 2001. **50**(2): p. 322-8.
41. Li, C., et al., *Elimination of K_{ATP} channels in mouse islets results in elevated [U-13C]glucose metabolism, glutaminolysis, and pyruvate cycling but a decreased gamma-aminobutyric acid shunt.* J Biol Chem, 2008. **283**(25): p. 17238-49.
42. Komatsu, H., et al., *Oxygen environment and islet size are the primary limiting factors of isolated pancreatic islet survival.* PLoS One, 2017. **12**(8): p. e0183780.
43. Mizumoto, H., et al., *Transient neonatal hyperinsulinism with adaptation disorders: a report of three cases.* J Pediatr Endocrinol Metab, 2015. **28**(3-4): p. 337-40.

44. Hoe, F.M., et al., *Clinical features and insulin regulation in infants with a syndrome of prolonged neonatal hyperinsulinism.* J Pediatr, 2006. **148**(2): p. 207-12.

Figure 1

A

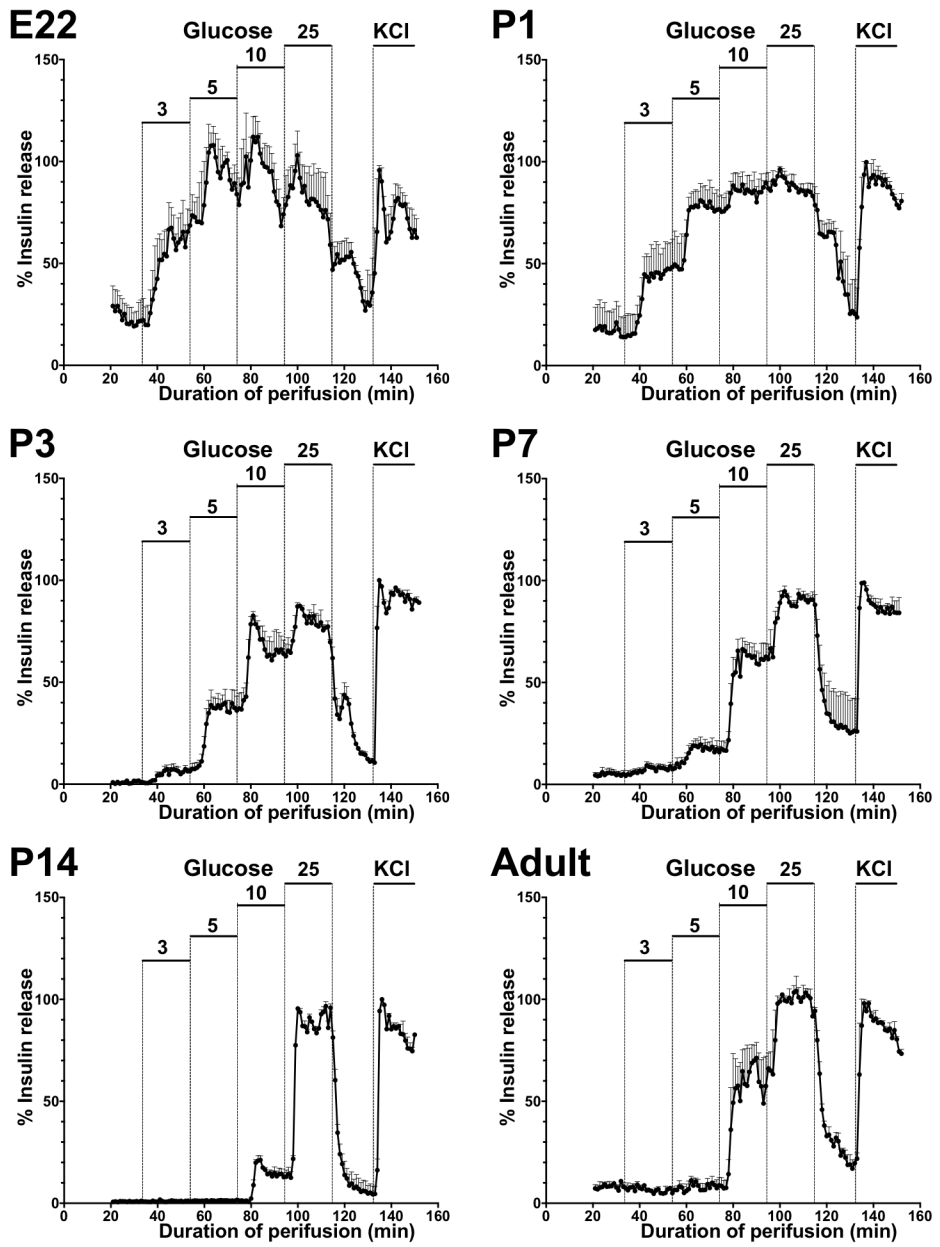
E22
P1
P3
P7
P14
Adult
Glucose
3
5
10
25
KCl
% Insulin release
Duration of perifusion (min)

B

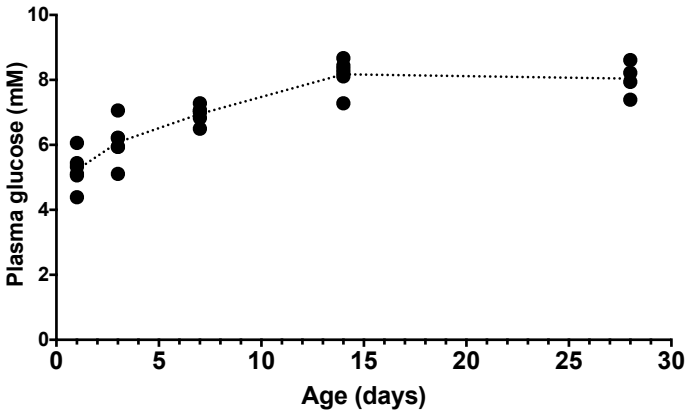
Plasma glucose (mM)
Age (days)

Figure 2

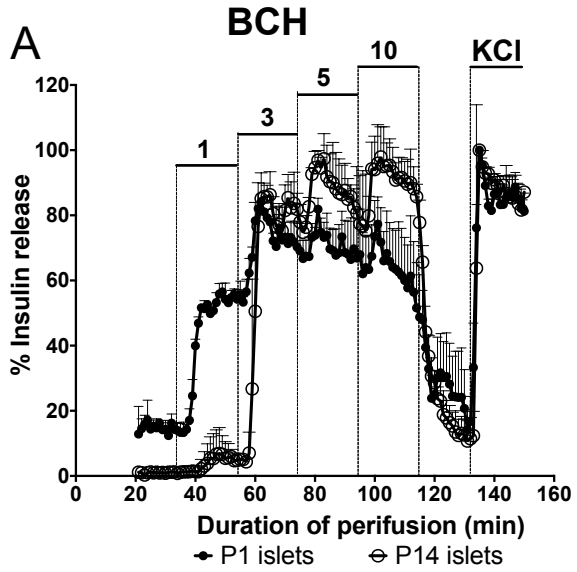
A
BCH
1
3
5
10
KCl
% Insulin release
Duration of perifusion (min)
P1 islets
P14 islets

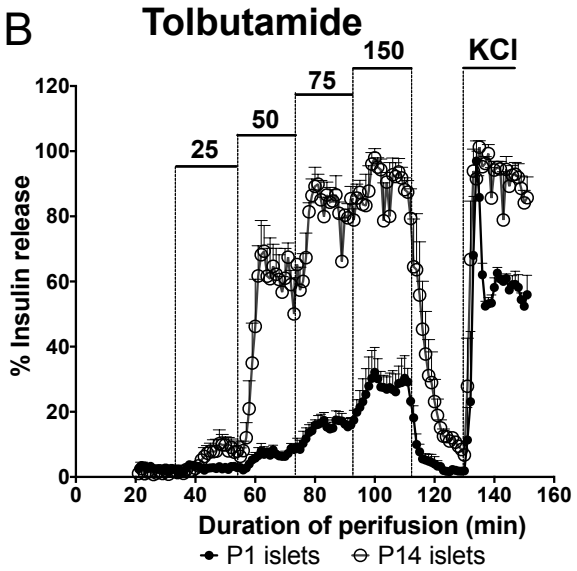
B
Tolbutamide
25
50
75
150
KCl
% Insulin release
Duration of perifusion (min)
P1 islets
P14 islets

Figure 3

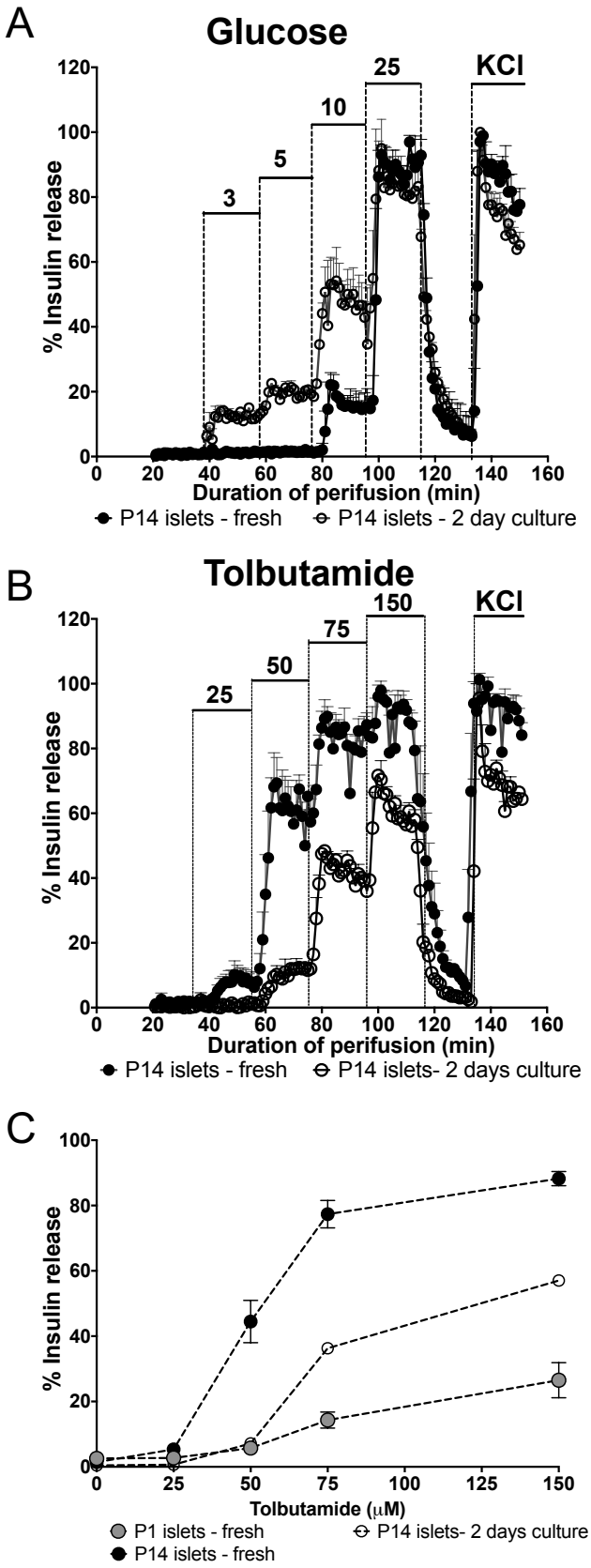
A
Glucose
3
5
10
25
KCl
% Insulin release
Duration of perifusion (min)
P14 islets - fresh
P14 islets - 2 day culture
B
Tolbutamide
25
50
75
150
KCl
% Insulin release
Duration of perifusion (min)
P14 islets - fresh
P14 islets- 2 days culture
C
% Insulin release
Tolbutamide (μM)
P1 islets - fresh
P14 islets - fresh
P14 islets- 2 days culture

Figure 4

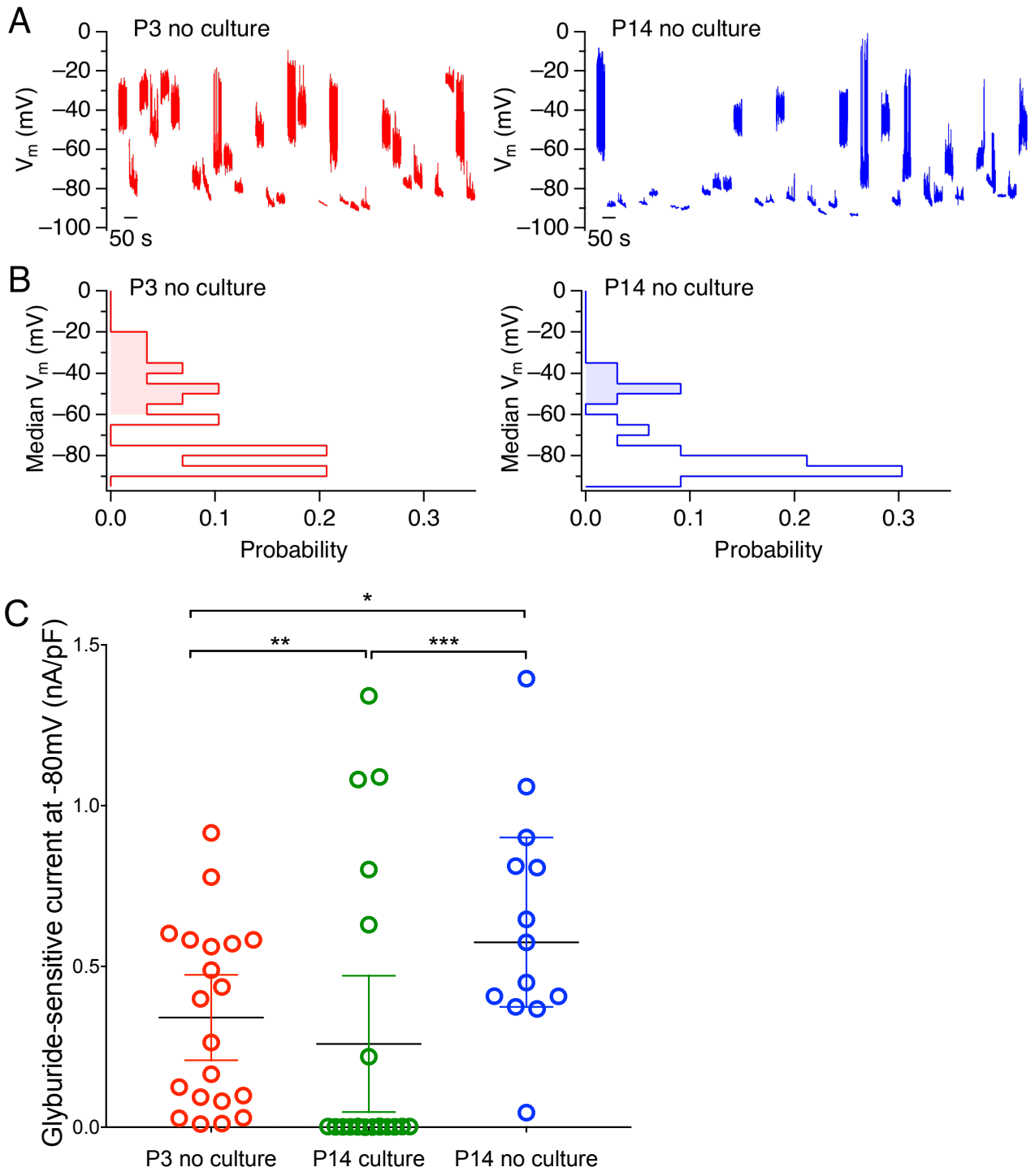
A
P3 no culture
P14 no culture
V_m (mV)
0
−20
−40
−60
−80
−100
50 s
B
P3 no culture
P14 no culture
Median V_m (mV)
0
−20
−40
−60
−80
0.0
0.1
0.2
0.3
Probability
C
Glyburide-sensitive current at -80mV (nA/pF)
1.5
1.0
0.5
0.0
*
**
***
P3 no culture
P14 culture
P14 no culture

Supplemental Figure 1

A

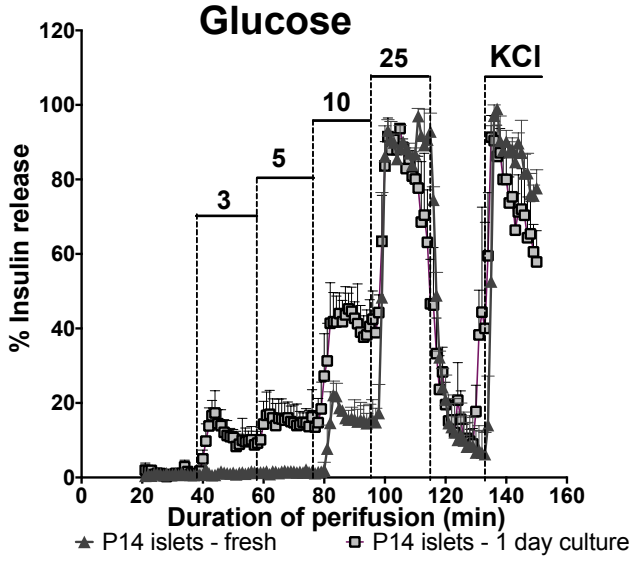

B

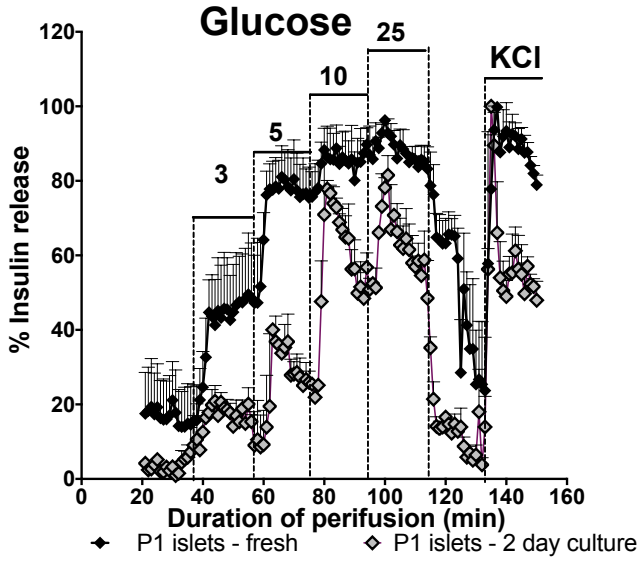

Supplemental Figure 2

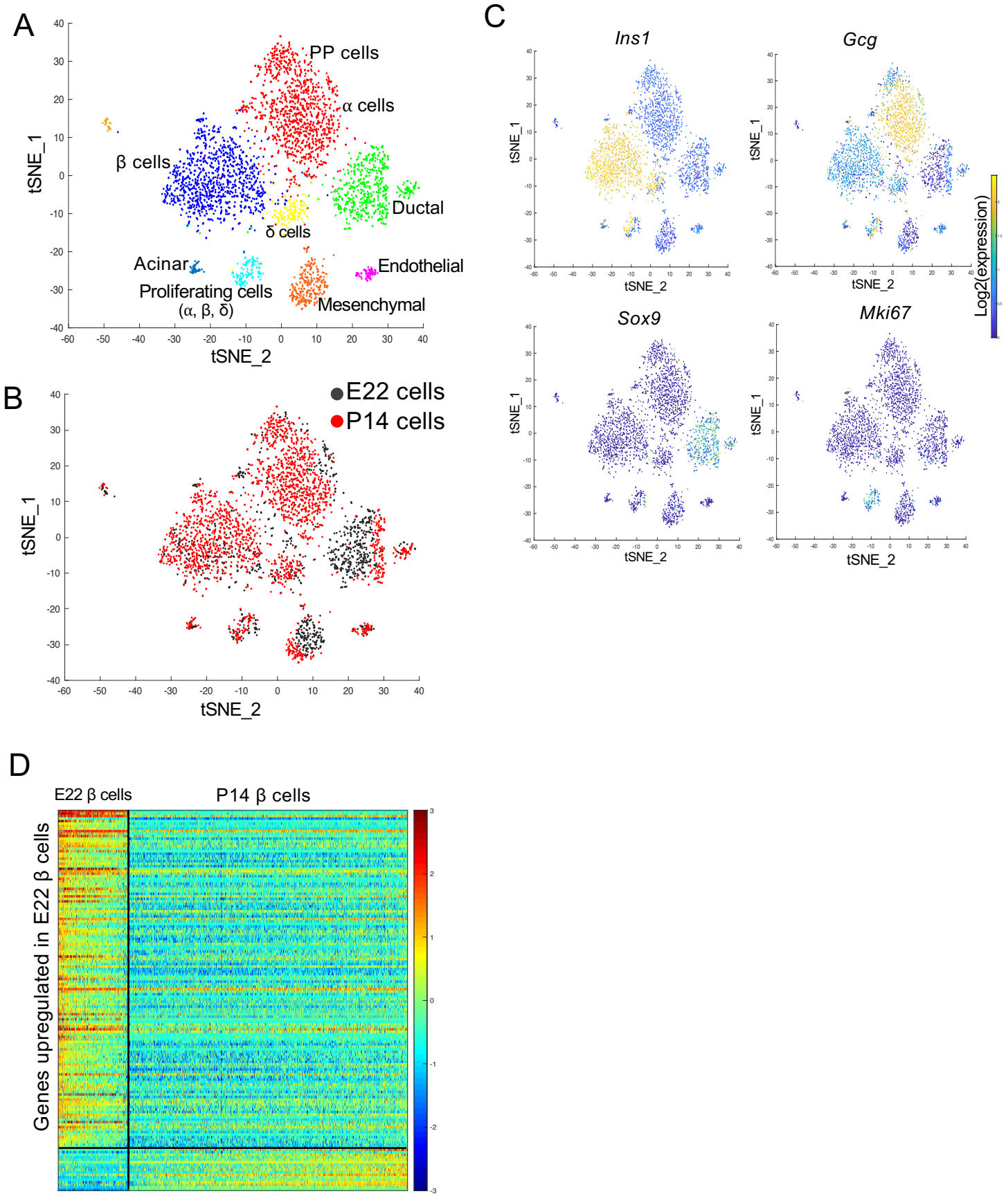

Supplemental Figure 2 - continued

E

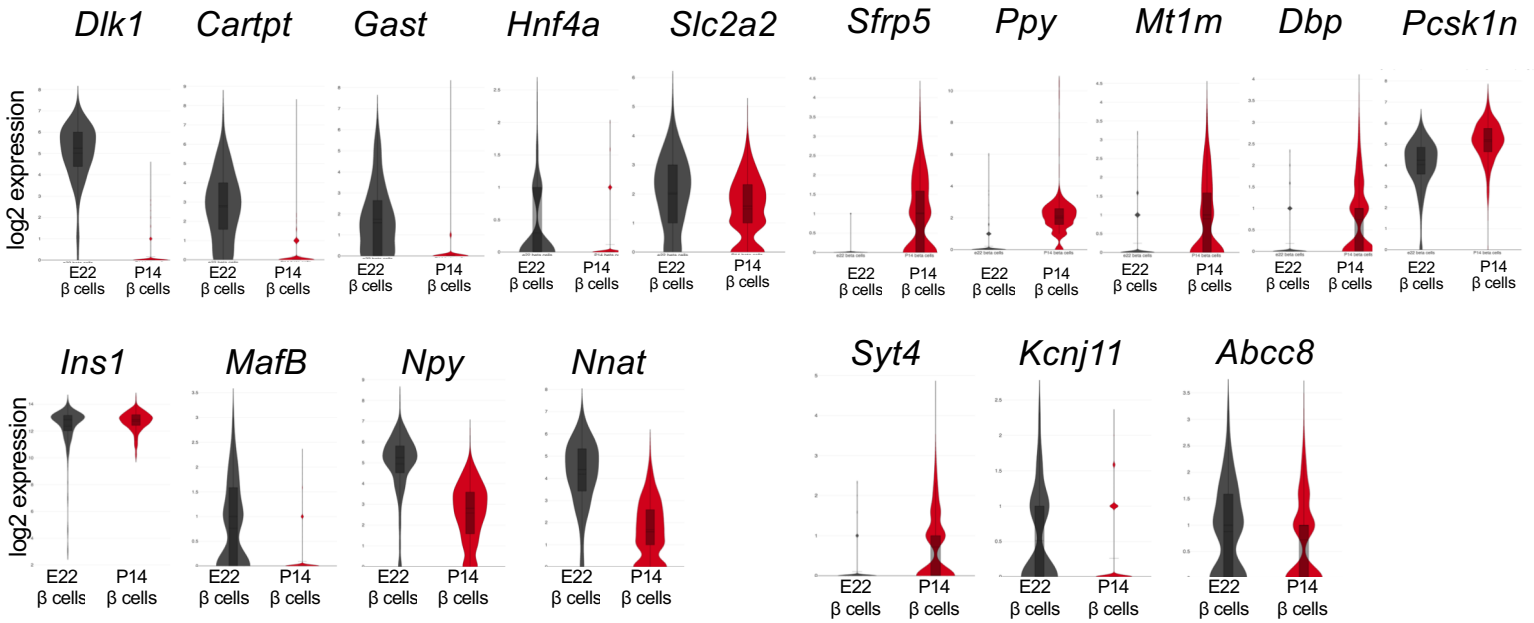

Supplemental Fig 3

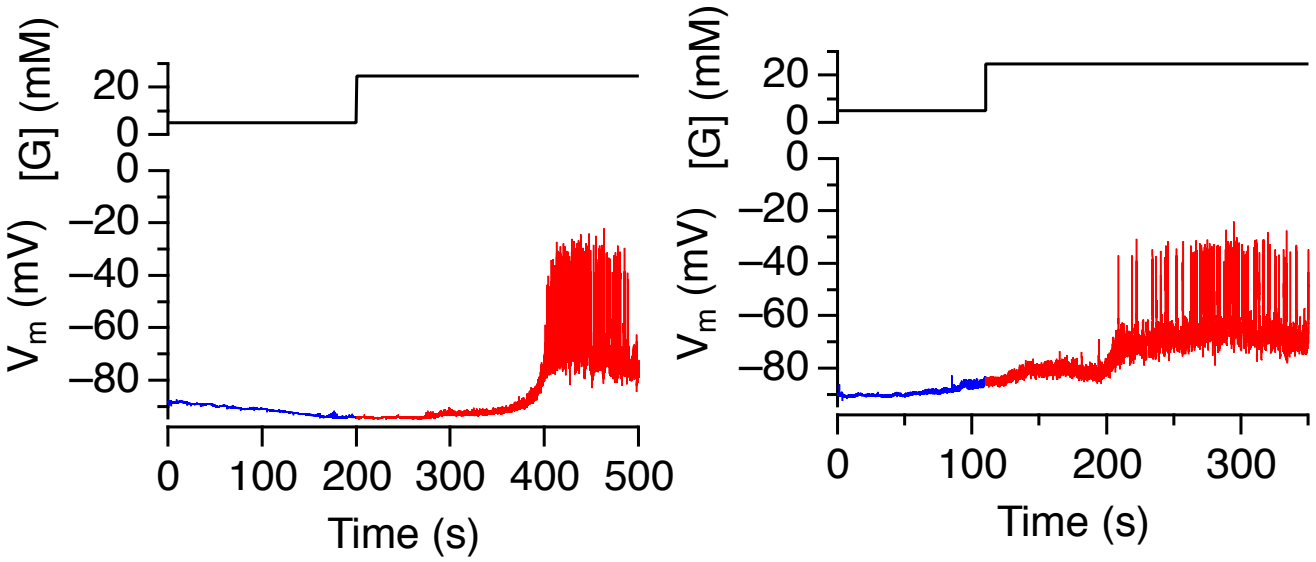

Supplemental Fig 4

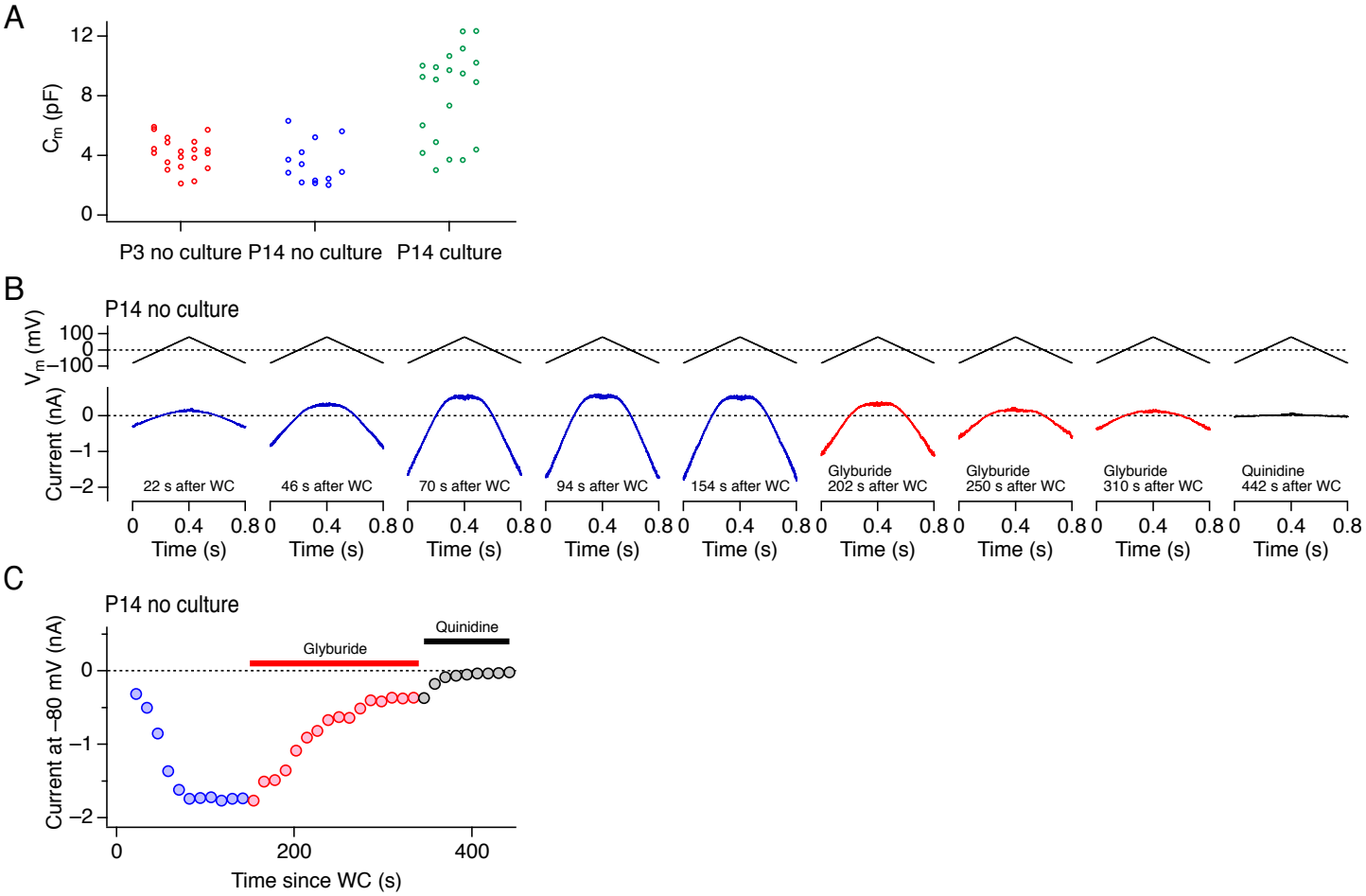

Supplemental Fig 5

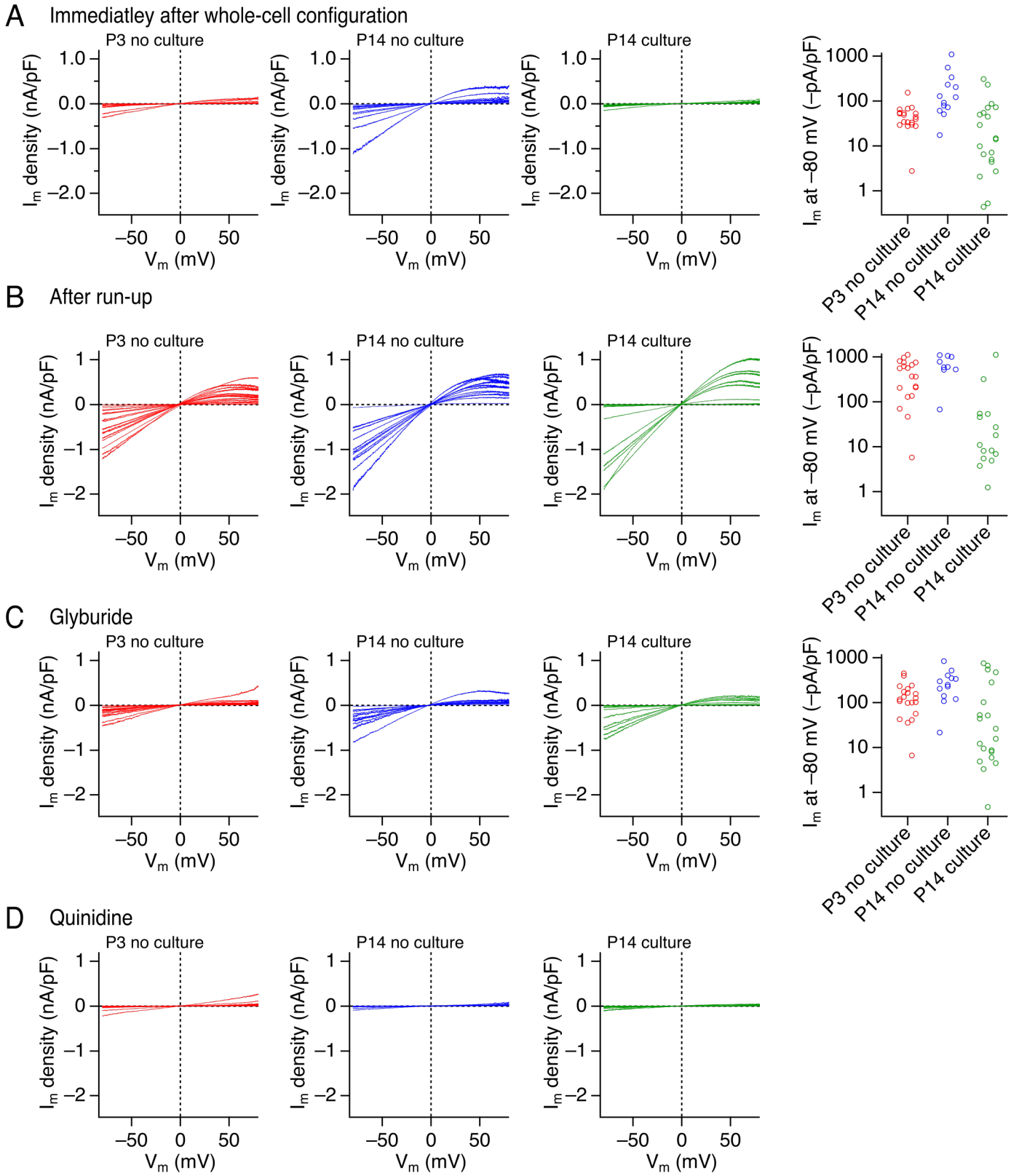

Supplemental Table: List of genes upregulated in E22 or P14 beta cells

Genes upregulated in E22 beta cells				Genes upregulated in P14 beta cells
Dlk1	*Msln*	*Amigo2*	*Cldn7*	*Syt4*
Cartpt	*LOC103694169*	*Crispld1*	*LOC100910944*	*Igfbp7*
Nnat	*Hist3h2ba*	*Erp29*	*Morf4l2*	*Sst*
Tmsb4x	*Myl6*	*F3*	*Rps27l*	*Insig1*
Gast	*Uqcr11*	*LOC100360791*	*Carhsp1*	*Errfi1*
Tmsbl1	*Calr*	*Cryba2*	*Shfm1*	*Pcsk1n*
Cd24	*LOC102551114*	*Uqcrq*		*LOC366502*
LOC680393	*Krt8*	*Usmg5*		*Bex1*
Npy	*Atp5i*	*LOC687780*		*Jund*
Hist1h2bh	*LOC108352861*	*Mafb*		*Rgs4*
Tff3	*Slc38a5*	*Ubl5*		*Ddit3*
RGD1560729	*Kcnk16*	*Edf1*		*Sepp1*
Cst6	*Psma4*	*LOC100911840*		*Sfrp5*
Pdia6	*Rpl10a*	*Psma7*		*Mt1*
Hsp90b1	*LOC363543*	*Atpif1*		*Mt2A*
Pyy	*LOC102548334*	*Pdia3*		*Ppy*
LOC689064	*RGD1561113*	*LOC100363869*		*Gcg*
Pfn1	*Pdcd5*	*Rpl38*		
Ndufa4	*Bsg*	*Atp5b*		
Lgals3	*Hspa5*	*Fkbp11*		
Tmsb10	*Prdx1*	*Gnb2*		
Ppib	*LOC100361558*	*Cox6a1*		
Dynll1	*Uqcr10*	*Smim22*		
LOC108349307	*LOC685154*	*LOC689574*		
Selm	*LOC690131*	*Maged2*		
C2cd4b	*Prdx2*	*LOC100911730*		
LOC690468	*Ap2s1*	*Atp5g3*		
Gcsh	*Ndufb7*	*C4bpb*		
Dstnl1	*Trh*	*Tceb2*		
Ssr2	*Card19*	*Rpn2*		
Txn1	*LOC108348144*	*Ostc*		
Pdia4	*RT1-A1*	*Nme2*		
RGD1566401	*Aplp1*	*LOC100362298*		
LOC108348891	*Nme1*	*Ndufa2*		
Hyou1	*Vcp*	*Ndufb11*		
LOC100912557	*Ywhah*	*P4hb*		
Creld2	*Tma7*	*B4galt6*		
Epcam	*LOC100359505*	*Gpx1*		
Atox1	*Pabpn1l*	*LOC102553447*		
Ifi27l2b	*Bud31*	*LOC100910996*		
Gpx3	*Lgals1*	*Fam234a*		
Gapdh	*Wfdc2*	*LOC103693132*		
Atp5j2	*Ssr4*	*Clic1*		